



Originally published as:

Biggin, A. J., Steinberger, B., Aubert, J., Suttie, N., Holme, R., Torsvik, T. H., van der Meer, D. G., van Hinsbergen, D. J. J. (2012): Possible links between long-term geomagnetic variations and whole-mantle convection processes. - *Nature Geoscience*, 5, 526-533

DOI: [10.1038/ngeo1521](https://doi.org/10.1038/ngeo1521)

1 **Possible links between long-term geomagnetic variations and whole-mantle convection**
2 **processes**

3 ***Biggin, A.J.^{a*}, Steinberger, B.^{b,c}, Aubert, J.^d, Suttie, N.^a, Holme, R.^a, Torsvik, T.H.^{c,ef}, van der***
4 ***Meer, D.G.^{g,h}, van Hinsbergen, D.J.J.^c***

5 *a. Geomagnetism Lab., Geology and Geophysics, School of Environmental Sciences, University*
6 *of Liverpool. L69 7ZE, UK*

7 *b. Helmholtz Centre Potsdam, GFZ German Research Centre for Geosciences, 14473 Potsdam,*
8 *Germany*

9 *c. Physics of Geological Processes, University of Oslo, Sem Saelands vei 24, 0316 Oslo, Norway*

10 *d. Institut de Physique du Globe de Paris, UMR7154, INSU, CNRS – Université Paris-Diderot,*
11 *PRES Sorbonne Paris Cité, 1 rue Jussieu, 75238 Paris cedex 5, France*

12 *e. Center for Geodynamics, Geological Survey of Norway (NGU), Leiv Eirikssons vei 39, 7491*
13 *Trondheim, Norway*

14 *f. School of Geosciences, University of the Witwatersrand, WITS 2050 Johannesburg, South*
15 *Africa*

16 *g. Institute of Earth Sciences, Utrecht University, Budapestlaan 4, 3584 CD Utrecht, The*
17 *Netherlands*

18 *h. Nexen Petroleum UK Ltd., Charter Place, UB8 1JG, Uxbridge, United Kingdom*

19 **Corresponding author: biggin@liv.ac.uk*

20

21 ***Preface***

22 The Earth's magnetic field is generated by convection in the liquid outer core that is modulated
23 by the pattern of heat flowing out into the base of the overlying mantle. Variations in
24 geomagnetic behaviour are observed on all timescales but those occurring over tens to
25 hundreds of millions of years may be related to changes in this heat flow caused by mantle
26 convection processes. These processes could also manifest themselves at the Earth's surface
27 through the medium of sinking lithospheric slabs and rising mantle plumes allowing
28 correlations to be made between palaeomagnetic behaviour and surface processes. Geodynamo
29 simulations suggest that transitions in geomagnetic behaviour from rapidly reversing to
30 superchron such as occurred between the mid-Jurassic and the mid-Cretaceous may have been
31 triggered by a decrease in core-mantle boundary heat flow globally or in the equatorial region.
32 Our synthesis indicates that this could have been related to a decrease in mantle plume head
33 production in the core-mantle boundary region, or to a major episode of true polar wander
34 occurring at that time, or to both. Further testing against quantitative modelling results and new
35 observations made for earlier times will be required to establish the robustness of such
36 intriguing links.

37

38 ***Main Text***

39 The Earth's magnetic field exhibits internally-driven variations on an extremely wide range of
40 timescales¹. As a highly nonlinear system, the geodynamo could produce all of these through a
41 stochastic process without the need to invoke any external forcing mechanism¹⁻³. For variations
42 observed on the timescale of tens to hundreds of Myr^{4,5}, however, the similarity to mantle
43 convection timescales suggests an alternative hypothesis whereby changes in core-mantle
44 boundary (CMB) heat flow play an important role in determining average geomagnetic
45 behaviour. This forcing could combine with an additional stochastic component of geodynamo

46 behaviour and is worthy of intense investigation because it could potentially allow geomagnetic
47 behaviour to be used to constrain lowermost mantle processes occurring over Earth's history.
48 An overarching theory of interaction could then be developed between the two great engines of
49 the Earth's interior: the geodynamo and mantle convection incorporating plate tectonics.

50 Based on the *a priori* acceptance of the mantle forcing hypothesis, numerous researchers have
51 causally related events in the palaeomagnetic and geological records⁶⁻¹⁹, linking, for example,
52 changes in magnetic polarity reversal frequency, via mantle plumes, to the emplacement of
53 large igneous provinces. Such claims are somewhat speculative but their general concept is
54 plausible. Interpretations of seismic wave tomography using global plate reconstructions
55 suggest that sinking lithospheric slabs and rising mantle plumes are indeed whole-mantle
56 processes^{20,21} conceivably influencing both the geodynamo and the surface. Furthermore,
57 numerical geodynamo models strongly support claims made by palaeomagnetists²²⁻²⁴, that
58 persistent non axial dipole features of the geomagnetic field observed over the last 10 kyr and
59 during individual excursions and reversals reflect the influence of the present-day pattern of
60 core-mantle heat flow^{25,26}. Mechanisms other than thermal interactions across the CMB could
61 also force the geodynamo on these and other timescales²⁷ but we shall not focus on these for the
62 purpose of this review.

63 Here we present a synthesis, using the latest results from a variety of disciplines, to examine
64 possible causal relationships between geomagnetic behaviour and mantle processes on the 10-
65 100 Myr timescale. We also highlight the future research required to test and develop these
66 links.

67 ***Geomagnetic variations on the 10-100 Myr timescale***

68 Two measures of geomagnetic behaviour are considered here: reversal frequency refers to the
69 average rate with which geomagnetic field flips from apparently stable normal to reverse
70 polarity and vice versa; dipole moment is the inferred strength of the dominant dipole
71 component of the geomagnetic field.

72 The Geomagnetic Polarity Time Scale (GPTS²⁸⁻³²; figure 1) indicates that reversal occurrence is a
73 stochastic process, but also provides unequivocal evidence that the average reversal frequency
74 has varied considerably over the last few hundreds of Myr⁵. Numerous statistical analyses of
75 this record have failed to produce a consensus on the underlying statistical distribution or
76 resolve whether a stationary dynamo process could produce such a time-dependent pattern of
77 reversal occurrence. We restrict our ourselves to investigating the coarsest (>30 Myr) timescale
78 variations as these are most readily explained in terms of mantle convection processes.

79 The earliest parts of the marine magnetic anomaly record (figure 1a) cannot be
80 straightforwardly interpreted in terms of a reversal sequence but continental
81 magnetostratigraphic studies suggest that anomalies back to at least 160 Ma are indeed
82 associated with reversals^{33,34}. Two periods in the last 200 Myr appear to represent examples of
83 the most extreme geomagnetic behaviour observed to date (figure 1). These are the mid-late
84 Jurassic (ca. 150-170 Ma) when reversal frequency peaked^{29,33}, possibly in excess of 12 Myr⁻¹,
85 and the Cretaceous Normal Superchron (CNS; 84-121Ma) when the field was almost exclusively
86 of single polarity for a period spanning nearly 40 Myr^{35,36}. In the late Cainozoic, some of the
87 polarity chrons are of shorter duration than have been documented at any earlier time. The
88 density of short (< 0.2Myr) chrons was clearly higher in the mid-Jurassic, however, leading to
89 higher average reversal frequency, even before considering that short duration chrons are more
90 likely to have been overlooked in earlier time periods.

91 Variations in the mean dipole moment through the Cretaceous and Cainozoic are still the subject
92 of vigorous debate³⁷⁻⁴¹ and good quality data from earlier times are sparse. Nonetheless,
93 measurements of dipole moment made from both whole-rock and single silicate crystals,
94 together with interpretations of the marine magnetic anomaly record, all suggest that the
95 average dipole moment was lower than average for at least part of the Jurassic period (140 –
96 200 Ma; figure 1b)^{6,29,38,42-46}.

97 Reversal frequency and dipole moment records suggest that there was a major transition in
98 geomagnetic behaviour between the mid-Jurassic (~170 Ma) and the mid-Cretaceous (~120
99 Ma; figure 1). Records of palaeosecular variation analysis, though based on limited data in the
100 case of the earlier time period, also support significantly different geomagnetic behaviour
101 during the Jurassic and mid-Cretaceous⁴⁷. It is still debated whether this transition from hyper-
102 reversal activity to superchron occurred over a short (~3 Myr) or much longer (~40 Myr) time
103 period^{2,48}.

104 Two earlier Phanerozoic superchrons have been claimed from continental magnetostratigraphic
105 records (see figure 1b): the Permo-Carboniferous Reversed Superchron (PCRS; ~265-310 Ma⁴⁹)
106 and the Ordovician Reversed Superchron (ORS; ~460-490 Ma⁵⁰). There is direct
107 magnetostratigraphic evidence that reversal frequency was very high (> 7-10 Myr⁻¹) just 10-20
108 Myr before the ORS in the mid-Cambrian^{51,52}. Magnetostratigraphic data are lacking prior to the
109 PCRS but preliminary measurements of the virtual dipole moment in the Devonian and Silurian
110 periods are lower than average⁶, similar to those in the Jurassic when reversal frequency was
111 high. Therefore, the CNS, PCRS, and ORS may all have been preceded by a period of reversal
112 hyperactivity. Interestingly, a further sharp transition from high reversal frequency to
113 superchron behaviour has also been reported from before the Phanerozoic in late
114 Mesoproterozoic (~1000-1060 Ma) rocks from southeastern Siberia⁵³.

115 In summary, palaeomagnetism supports geomagnetic variations occurring on the 10-100 Myr
116 timescale throughout the Phanerozoic and possibly also in the Precambrian. Furthermore,
117 figure 1b suggests some periodicity in the reversal record, each superchron separated by a
118 period of 180-190 Myr..

119

120 **Sensitivity of the geodynamo to changes in CMB heat flow**

121 To understand how geomagnetic variations could be related to changes in CMB heat flow, we
122 turn to insights provided by dynamo theory. Numerical geodynamo models provide powerful

123 tools with which to study geomagnetic variations on all timescales but, because the parameters
124 at which numerical dynamos can be operated differ enormously from those of the Earth's core,
125 systematic exploration of parameter space is necessary. In particular, the very large disparity
126 between the typical diffusion times of the core momentum, magnetic field and buoyancy
127 anomaly, and the ratios of all these times with respect to an Earth day, must all be greatly
128 reduced in the models to maintain a tractable problem size²⁵.

129 Since fluid flow in the outer core (measured in mm/s) is so much faster than mantle flow
130 (measured in mm/year), the geodynamo is sensitive to the “instantaneous” heat flow conditions
131 imposed by the mantle rather than its rate of change on mantle timescales. The geodynamo is
132 largely driven by compositional convection produced by the release of light elements at its base
133 rather than thermal convection caused by cooling from the top. Nonetheless, this process is still
134 dependent on, and modulated by, the heat flowing out of the core at a rate dictated by
135 conditions in the lowermost mantle.

136 To first order, reversal frequency appears to be positively correlated to CMB heat flow:
137 enhancing convection in dynamo simulations by increasing this flow tends to destabilise the
138 dipole generation process making reversals more likely⁵⁴⁻⁵⁷ though maintaining a stochastic
139 pattern⁵⁶. Reversing dynamos require high forcing and long simulation times for a significant
140 statistical assessment, however, making extensive parametric studies difficult⁵⁸.

141 The evolution of reversal frequency has been linked to a local version of the Rossby (Ro)
142 number (the ratio of inertial to rotational forces), which is specific to a typical length scale of the
143 fluid flow^{54,55,59,60}. An empirically derived relationship^{54,59} suggests that the local Ro scales as the
144 square root of the power available to drive the dynamo (which increases with CMB heat flow).
145 Results from a simple numerical dynamo model⁵⁵ suggests that a twofold increase of the local
146 Ro number (associated with a fourfold increase in dynamo power according to the scaling
147 relationship) is sufficient to drive the dynamo from a state where reversals first occur to a state
148 where they occur frequently at an average rate of about 10 per million year. Accounting for the

149 affine relationship between dynamo power and CMB heat flow⁵⁴, this increase in the reversal
150 frequency can, for example, be achieved if the CMB heat flow varies from 4 TW to 12 TW, in a
151 system where the core adiabatic heat flow is 6 TW, or from 9 to 20 TW in a system where the
152 adiabatic heat flow is 15 TW⁶⁰.

153 When increasing the CMB heat flow beyond the point where reversals start the magnetic field
154 strength may decrease. Results from a simple numerical dynamo model⁵⁵ suggest that a twofold
155 increase in the CMB heat flow could reduce the dipole moment by half. Assuming that the
156 geodynamo lies close to such a transition^{55,61}, a period of dynamo hyperactivity (high reversal
157 frequency) - caused by high CMB heat flow - may be associated with a low dipole moment and a
158 period of low dynamo activity (superchron) - caused by low CMB heat flow - may be
159 characterised by a high dipole moment⁵⁶. This is consistent with the combination of low dipole
160 moment and high reversal frequency measured in the Jurassic. The opposite combination (high
161 dipole moment, no reversals) is suggested by some data⁴⁵ during the Cretaceous Superchron
162 (figure 1b) and would also fit this prediction.,

163 Changes in the spatial pattern of CMB heat flow alone may also exert a strong effect on reversal
164 frequency^{26,62}. It has been argued⁶³ that increasing the heterogeneity of the CMB heat flow, while
165 holding the net heat flow at a constant value, also tends to decrease the stability of the dynamo
166 producing more reversals. Due to the nature of its columnar convection, the geodynamo is
167 expected to be mostly influenced by low-latitude heat-flow variations²⁵ and this sensitivity has
168 been highlighted in a numerical model study⁶³ in which many more reversals occurred when the
169 low-latitude heat flow was increased. Using a mechanism developed from a low-order dynamo
170 model⁶⁴, it has also been argued that the equatorial asymmetry in CMB heat flow has strongly
171 influenced reversal frequency: reversals becoming more common when the north-south
172 symmetry is broken¹⁴.

173 Intriguingly, the outputs of some heterogeneously forced models⁶³ appear not to produce a
174 simple inverse relationship between measured average reversal frequency and mean axial

175 dipole moment. If confirmed as a robust prediction of geodynamo theory, a decoupling of these
176 parameters under certain heterogeneous boundary conditions could provide an explanation,
177 alternative to low measurement fidelity⁴⁰, for the apparent small change in mean dipole
178 moment since the mid-Cretaceous (figure 1b).

179 Overall, dynamo theory supports the hypothesis that the geomagnetic variability outlined in the
180 previous section could be caused by changes in the magnitude and/or spatial pattern of heat
181 flow across the CMB, with higher heat flow (particularly in equatorial zones) and greater
182 heterogeneity in its pattern both producing more reversals. Though significant variations in
183 chron length have been observed to occur spontaneously in a long running dynamo
184 simulation⁶⁵, those of the magnitude observed in the palaeomagnetic record have not been
185 reproduced without forcing⁵⁶. To our knowledge, no geodynamo modelling studies have yet
186 explicitly tested how the effects of changing the global net heat flow differ in the cases of
187 homogeneous versus heterogeneous boundary conditions. As the following section makes clear,
188 this is urgently required to understand how long timescale geomagnetic variations might arise.

189

190 ***CMB heat flow and its potential variability on the 10-100 Myr timescale***

191 Heat flow from the core into the mantle is proportional to the temperature contrast across the
192 thermal boundary layer (TBL) at the base of the mantle, the thermal conductivity of the
193 lowermost mantle, and inversely proportional to the TBL's thickness. All of these quantities,
194 however, are rather uncertain and therefore estimates of present-day heat flow are widely
195 discrepant (though mostly in the range 5-15 TW⁶⁶; 33-100 mWm⁻²). Seismological studies
196 suggest a high degree of heterogeneity in the lowermost mantle⁶⁷ which corresponds to large
197 variations in local heat flow. In particular, two approximately antipodal large low shear-wave
198 velocity provinces (LLSVPs) span thousands of km under Africa and the central Pacific, and are
199 thought to represent intrinsically dense thermochemical piles that may be associated with very
200 low CMB heat flow⁶⁸.

201 CMB heat flow is likely to be variable on mantle convection timescales¹⁵. The TBL may be
202 influenced by subducted slabs in the lower mantle, by mantle plumes departing from the CMB,
203 and by the distribution of the thermochemical piles in the lowermost mantle. Furthermore,
204 episodes of true polar wander (TPW) effectively rotate the entire pattern of CMB heat flow with
205 respect to the dominant time-averaged flow structures in the outer core.

206 Mantle flow models constrained by plate reconstructions at their upper boundary can be used
207 to infer the history of CMB heat flow and its relationship with subduction history¹⁵. This
208 approach is applied here using an independent set of mantle flow models with a somewhat
209 different radial viscosity profile, subduction history, and model parameters than previous
210 efforts (see supplementary information for details). These models mostly support a large spatial
211 variation in the amplitude of CMB heat flux. Beneath thermochemical piles (mostly red-white
212 colours in figure 2c), it is much lower ($< 40 \text{ mWm}^{-2}$) than where subducted slab remnants
213 overlie the CMB ($150\text{-}250 \text{ mWm}^{-2}$)¹⁵. Reconstructed positions of large igneous provinces and
214 kimberlites suggest that the thermochemical piles have covered similar areas of the CMB for
215 over 500 million years²⁰. Large variations in CMB heat flow must therefore have occurred
216 elsewhere.

217 Our mantle flow models mostly produce high total CMB heat flow ($> 10 \text{ TW}$) as may be required
218 to maintain the geodynamo⁶⁰. Case 2A (using the output of Case 2 at 0 Myr as the initial
219 condition) in figure 2 is the closest to equilibrium and produces temporal variations in total
220 CMB heat flow on the order of a few tens of percent over the last few hundreds of Myr (see also
221 the supplementary movie). According to the empirical scaling relationship^{54,59} mentioned
222 earlier, relative changes of this magnitude would probably be insufficient to drive significant
223 changes in the reversal behaviour of a homogeneously forced dynamo⁵⁴. The boundary
224 conditions for the geodynamo are probably far from the homogeneous state used to construct
225 this relationship, however, and dynamo models also supports changes in magnetic behaviour
226 forced purely by changes in the pattern of heat flow even when no net variation occurs^{26,62,63}.

227 Therefore, we must conclude that, although the concepts under review here presently lack
228 quantitative support, the possibility that changes in CMB heat flow do affect the geodynamo
229 cannot yet be rejected. The highly nonlinear nature of the geodynamo could plausibly amplify
230 even relatively minor shifts in forcing to produce major transitions in geomagnetic behaviour.

231 **Potential links between geomagnetic behaviour and subduction activity**

232 Numerous studies have attempted to relate the distribution of subduction zones and inferred
233 subduction rates to variations in geomagnetic behaviour. Some of their hypotheses^{6,9,69} now
234 appear unlikely because they assume that increasing net CMB heat flow decreases reversal
235 frequency (and increases mean dipole moment), the opposite relationship to that implied by the
236 dynamo models. Others^{10,14} do invoke more plausible relationships between CMB heat flow and
237 dynamo behaviour but allow no time lag in transferring information between the crust and core.

238 Sinking lithospheric slabs can stagnate temporarily on top of the 660-km discontinuity⁷⁰, but
239 they eventually sink into the lower mantle⁷¹⁻⁷⁴. Sinking slabs displace material ahead of them
240 thinning the TBL and increasing CMB heat flow long before they actually reach the lowermost
241 mantle⁷⁵. By running some of our models with zero subduction flow before and after the 0-300
242 Ma period for which the plate history is constrained, the time delay associated with the
243 response of CMB heat flow to slab input was explored. The models showed an initial response to
244 subduction initiation after a delay of approximately 50 Myr (figure 2a). By contrast, the time
245 between subduction cessation and heat flow decrease at the location where the slab perturbed
246 CMB heat flow can be 250 Myr or longer as the slab sinks and is subsequently warmed (figure
247 2). Similarly, a study that coupled tomography to plate reconstructions found a survival time for
248 slabs of ~250-300 Myr²¹.

249 Some mantle models¹⁵ have produced weak minima in the equatorial heat flow at times (ca. 100
250 Ma and 270 Ma) that fall within the CNS and PCRS. This, combined with an apparent sensitivity
251 of dynamo models⁶³ to variations in this parameter, has been offered as a potential explanation
252 for the occurrence of these superchrons¹⁵. Our models do not all support a minimum in

253 equatorial CMB heat flow at the time of the last superchron, however (see the supplementary
254 information).

255 A more robust observation based on our analysis is that equatorial asymmetry increased from a
256 minimum in the Cretaceous as subduction flux in the northern hemisphere increased relative to
257 that in the south (see figure 2c and supplementary figure 1). This suggests that increasing
258 north-south asymmetry in heat flow might have played a role in increasing reversal frequency
259 through the late Cretaceous and Cainozoic¹⁴ though the required sensitivity of the dynamo
260 remains to be established.

261 It has been argued¹⁵ that the onset of the PCRS was essentially caused by the cessation of
262 subduction associated with the collision of Laurussia and Gondwana approximately 20 Myr
263 earlier at 330 Ma. It is, however, not clear how this could fit with our findings of a long drawn-
264 out response of CMB heat flow to subduction cessation (figure 2). Variability in slab sinking
265 speeds⁷⁶ and CMB heat flow response time (figure 2) imply that establishing robust correlations
266 between geomagnetic behaviour and subduction events may prove difficult.

267 **Potential links between geomagnetic behaviour and mantle plume activity**

268 Deep mantle plumes, rising from the lowermost mantle, remove hot material from the TBL
269 increasing the local CMB heat flow. This increase may be only a minor effect relative to the heat
270 flow variations caused by the arrival of cold slabs above the CMB, however⁷⁷⁻⁷⁹. Our numerical
271 model contains both slabs and plumes and supports that the departure of plume heads from the
272 TBL is itself modulated to some degree by slab arrival. The margins of the thermochemical piles
273 have been referred to as 'plume-generation zones' where plumes appear to form
274 preferentially^{20,80,81}. Here, slabs can act as a 'pushbroom', sweeping up material into upwellings
275 over the margins of the piles^{75,79,82,83} (see supplementary figure 3). Therefore, plume head
276 departure from the CMB may be associated with an increase in heat flow there even if it does
277 not directly cause it; the effects of slabs and plumes on CMB heat flow cannot easily be
278 separated.

279 Early attempts to link mantle plume activity (expressed in the geological record as large igneous
280 province and kimberlite formation) to magnetic reversal frequency claimed that plumes caused
281 superchrons¹¹⁻¹³. The mid-late Cretaceous was indeed a time of both major intra-plate
282 volcanism likely sourced by mantle plumes^{20,84} and unusually low geomagnetic reversal
283 frequency, but it now appears unlikely that these two specific phenomena are directly related in
284 the manner claimed. Dynamo models imply that plumes, and the increase in CMB heat flow they
285 represent, are more likely to be associated with periods of elevated rather than suppressed
286 reversal frequency^{54,56,63}. Also, enhanced Cretaceous LIP activity in both the African and Pacific
287 hemispheres was apparently underway before the superchron even began⁸⁵, which would not
288 allow time for the plumes to rise through the mantle.

289 It has also been claimed that the three Phanerozoic superchrons were each terminated by the
290 departure of a plume head from the CMB which then manifested itself in a LIP at the Earth's
291 surface some 10-20 Myr later⁸. Such a short time lag works well for explaining superchron
292 termination but leaves superchron onset unexplained and, assuming the same rise time, the
293 mid-Cretaceous pulse of LIP activity uncorrelated with reversal frequency. Estimates for plume
294 rise-time from the CMB to the surface vary between 5 and 100 Myr^{86,87} with recent modelling⁸⁸
295 favouring 20-50 Myr. Taking the upper limit of 50 Myr suggests a broadly positive correlation
296 between LIP activity and reversal frequency on the time range 50-200 Myr (see figure 3) and
297 one that is also consistent with our first-order understanding of how the geodynamo is likely to
298 respond to changes in CMB heat flow.

299 The correlation in figure 3 may prove to be fortuitous or to be valid only for certain time
300 periods. Taken at face value, however, the elevated reversal frequency observed for the last 30-
301 40 Myr could imply that several plume heads left the CMB since that time and are now rising
302 through the mid-mantle. Consequently, if this correlation could be made robust through a
303 greater understanding of the mantle plume head generation and rise process, as well as the

304 geodynamo's response to the resulting changes in CMB heat flow, the palaeomagnetic record
305 could, in the future, perhaps help predict plume activity at the surface.

306

307 **Potential links between geomagnetic behaviour and true polar wander**

308 The Earth's spin axis tends to align with the maximum non-hydrostatic inertia axis imposed by
309 mantle density anomalies (including slabs, plumes and thermochemical piles) through "true
310 polar wander" (TPW), a re-orientation of the entire Earth's mantle and crust relative to the spin
311 axis⁸⁹. The large-scale orientation of the outer core fluid motion is dictated by the spin axis and
312 therefore the main effect of TPW on the geodynamo is to change the pattern of heat flow across
313 the CMB with respect to it. It is these changes in heat flow boundary conditions, rather than the
314 rotations themselves, that possibly influence geomagnetic behaviour. TPW occurs at a rate
315 determined by mantle viscosity of probably $< \sim 1\text{-}2$ deg/Myr^{90,91} and observations indicate that
316 during the past 300 Myr, TPW has moved the pole up to $\sim 23^\circ$ from its present location, roughly
317 in a plane such that the two thermochemical piles beneath Africa and the Pacific remain close to
318 the equator⁹².

319 Except for one early study⁷, little attention has been paid to how reported episodes of TPW
320 could have influenced geomagnetic field behaviour. Presuming that the stability of the
321 geodynamo is indeed sensitive to the spatial pattern of heat flow (and equatorial heat flow in
322 particular), it could, however, be very important.

323 The effect (described by a kernel function) that density anomalies at different depths within the
324 mantle have on the Earth's moment of inertia is likely to be such that TPW will tend to place
325 dense slabs in the upper and upper-mid mantle at low latitudes and those in the lowermost
326 mantle at higher latitudes⁹⁰. The reverse is true of rising plume heads of low density. Because of
327 these mutual compensations, it is difficult to obtain a good agreement between modelled and
328 observation-based TPW and results presented in figure 2 and supplementary figure 1 therefore

329 do not consider the TPW that would follow from these models. Qualitatively, the combined
330 effect of any major perturbation to subduction and/or plume flux (produced by e.g.
331 supercontinent formation or breakup) that affects the degree 2 component of the geoid would
332 be to cause patches of thinned TBL (elevated heat flux) produced by either slabs and/or plumes
333 to move first towards the equator, and then towards the poles. We provide an exaggerated
334 demonstration of this process in figure 4 which shows the response of the CMB heat flow in an
335 equatorial zone (given as a fraction of the total heat flow) to episodes of TPW resulting from
336 subduction being switched “on” and “off” in the model. After a delay of approximately 100 Myr,
337 both of these perturbations cause episodes of TPW that produce dramatic rises and then falls in
338 the equatorial heat flow. Coupled to a sensitivity of the geodynamo to equatorial heat flow, this
339 general process might implicate episodes of TPW as a contributor to observed episodes of
340 reversal hyperactivity followed by superchrons in the palaeomagnetic record. Various dramatic
341 episodes of TPW claimed for the early Phanerozoic and Proterozoic⁹³ have been linked to the
342 supercontinent cycle and could correspond to the earlier, relatively rapid, transitions in
343 geomagnetic behaviour (figure 1b)^{50,53} mentioned previously. More palaeomagnetic data from
344 around these intervals would be useful to test this link.

345 Figure 5 shows the results of a simple analysis that applies four recently outlined episodes of
346 TPW^{92,94} for the period 100-250 Ma to the SMEAN seismic tomography model at a depth slice of
347 2850 km⁹⁵. Assuming that the shear wave velocity anomaly at this depth can be used to infer
348 variations in CMB heat flow⁶³, we find that, even in the absence of any temporal CMB variations
349 in the mantle reference frame, the TPW rotations would have produced changes in equatorial
350 heat flow that relate reasonably well in sign, relative amplitude, and timing to those required to
351 cause the observed geomagnetic changes in the same period. The same rotations applied to an
352 output of a mantle flow model cause substantial changes (up to 40% for the $\pm 10^\circ$ latitude zone)
353 in the equatorial heat flow (see supplementary information). We therefore conclude that,
354 subject to the necessary sensitivity of the geodynamo being confirmed, TPW could well have
355 contributed to changes in geomagnetic behaviour over this time period - particularly the

356 reduction of reversal frequency and increase in mean dipole moment observed between the
357 mid-Jurassic and mid-Cretaceous.

358 **Summary and Outlook**

359 Transitions in geomagnetic behaviour manifested primarily as decreases in average reversal
360 frequency preceding superchrons may be caused by reductions in CMB heat flow globally, or in
361 the equatorial region. The most recent such transition occurring between the mid-Jurassic and
362 mid-Cretaceous coincided with a major TPW event that probably moved patches of high heat
363 flow away from the equator. It may also have been associated with a decline in average mantle
364 plume head production rate at the CMB that could have signified a decrease in the net heat flow
365 across that boundary. The most recent long term increase in average reversal frequency since
366 the late Cretaceous may have been caused by increasing equatorial asymmetry in CMB heat flow
367 or another subduction-related process that triggered the departure of plume heads that have
368 not yet reached the surface. These and other correlations are not mutually exclusive; slabs,
369 plumes, dense basal piles, and TPW are all interrelated elements of mantle convection^{75,90,96}.
370 This interrelation may provide any future successful overarching hypothesis with the
371 opportunity to unify numerous different components of the core-mantle-crust system while
372 taking into account the time lags implicit between them.

373

374 The correlations outlined above fit with our qualitative understanding of how the geodynamo is
375 likely to respond to CMB heat flow changes but are otherwise not yet robust. More
376 comprehensive and realistic modelling studies aimed at better-constraining the history of CMB
377 heat flow and the geodynamo's sensitivity to possible changes in it are required in the future.
378 Furthermore, the generic links outlined here should be tested using palaeomagnetic data
379 describing geomagnetic behaviour and palaeogeography (including the position of the rotation
380 axis) during earlier time periods.

381

382 All correspondence and requests for materials should be addressed to AB (biggin@liv.ac.uk)

383

384 **Acknowledgements:** AB is funded by a NERC Advanced Fellowship (NE/F015208/1). NS, AB,
385 and RH are funded by a NERC standard grant (NE/H021043/1). AB acknowledges valuable
386 discussions with Neil Thomas and Mimi Hill. JA acknowledges support from program PNP/SEDI-
387 TPS of French Institut National des Sciences de l'Univers (INSU). THT acknowledges the
388 European Research Council for financial support.

389 **Author Contributions:** AB, BS, and JA prepared the text with contributions from all other
390 authors. BS supplied the mantle modelling results and JA the geodynamo modelling results. New
391 analyses were performed by AB and BS. All authors contributed to discussions about the ideas
392 presented.

393 **References**

- 394 1 Jonkers, A. R. T. Discrete scale invariance connects geodynamo timescales. *Geophys J Int*
395 **171**, 581-593 (2007).
- 396 2 Hulot, G. & Gallet, Y. Do superchrons occur without any palaeomagnetic warning? *Earth*
397 *Planet Sc Lett* **210**, 191-201 (2003).
- 398 3 Jonkers, A. R. T. Long-range dependence in the Cenozoic reversal record. *Phys Earth Planet*
399 *In* **135**, 253-266 (2003).
- 400 4 Jones, G. M. Thermal interaction of the core and the mantle and long-term behavior of the
401 geomagnetic field. *J Geophys Res* **82**, 1703-1709 (1977).
- 402 5 Mcfadden, P. L. & Merrill, R. T. Lower Mantle Convection and Geomagnetism. *J Geophys Res*
403 **89**, 3354-3362 (1984).
- 404 6 Biggin, A. J. & Thomas, D. N. Analysis of long-term variations in the geomagnetic poloidal
405 field intensity and evaluation of their relationship with global geodynamics. *Geophys J Int*
406 **152**, 392-415 (2003).
- 407 7 Courtillot, V. & Besse, J. Magnetic-Field Reversals, Polar Wander, and Core-Mantle Coupling.
408 *Science* **237**, 1140-1147 (1987).
- 409 8 Courtillot, V. & Olson, P. Mantle plumes link magnetic superchrons to Phanerozoic mass
410 depletion events. *Earth Planet Sc Lett* **260**, 495-504 (2007).
- 411 9 Eide, E. A. & Torsvik, T. H. Paleozoic supercontinental assembly, mantle flushing, and genesis
412 of the Kiaman Superchron. *Earth Planet Sc Lett* **144**, 389-402 (1996).
- 413 10 Gaffin, S. Phase Difference between Sea-Level and Magnetic Reversal Rate. *Nature* **329**, 816-
414 819 (1987).
- 415 11 Haggerty, S. E. Superkimberlites - a Geodynamic Diamond Window to the Earths Core. *Earth*
416 *Planet Sc Lett* **122**, 57-69 (1994).
- 417 12 Larson, R. L. & Kincaid, C. Onset of mid-Cretaceous volcanism by elevation of the 670 km
418 thermal boundary layer. *Geology* **24**, 551-554 (1996).

419 13 Larson, R. L. & Olson, P. Mantle plumes control magnetic reversal frequency. *Earth Planet Sc*
420 *Lett* **107**, 437-447 (1991).

421 14 Pétrélis, F., Besse, J. & Valet, J.-P. Plate tectonics may control geomagnetic reversal
422 frequency. *Geophys Res Lett* **38**, doi:10.1029/2011GL048784 (2011).

423 15 Zhang, N. & Zhong, S. J. Heat fluxes at the Earth's surface and core-mantle boundary since
424 Pangea formation and their implications for the geomagnetic superchrons. *Earth Planet Sc*
425 *Lett* **306**, 205-216, doi:10.1016/j.epsl.2011.04.001 (2011).

426 16 Ricou, L. E. & Gibert, D. The magnetic reversal sequence studied using wavelet analysis: a
427 record of the Earth's tectonic history at the core-mantle boundary. *Cr Acad Sci II A* **325**, 753-
428 759 (1997).

429 17 Vogt, P. R. Evidence for Global Synchronism in Mantle Plume Convection, and Possible
430 Significance for Geology. *Nature* **240**, 338-& (1972).

431 18 Jones, G. M. Thermal Interaction of Core and Mantle and Long-Term Behavior of
432 Geomagnetic-Field. *J Geophys Res* **82**, 1703-1709 (1977).

433 19 Loper, D. E. & Mccartney, K. Mantle Plumes and the Periodicity of Magnetic-Field Reversals.
434 *Geophys Res Lett* **13**, 1525-1528 (1986).

435 20 Torsvik, T. H., Burke, K., Steinberger, B., Webb, S. J. & Ashwal, L. D. Diamonds sampled by
436 plumes from the core-mantle boundary. *Nature* **466**, 352-U100 (2010).

437 21 van der Meer, D. G., Spakman, W., van Hinsbergen, D. J. J., Amaru, M. L. & Torsvik, T. H.
438 Towards absolute plate motions constrained by lower-mantle slab remnants. *Nat Geosci* **3**,
439 36-40 (2010).

440 22 Constable, C. G. Modelling the geomagnetic field from syntheses of paleomagnetic data.
441 *Phys Earth Planet In* **187**, 109-117 (2011).

442 23 Korte, M. & Holme, R. On the persistence of geomagnetic flux lobes in global Holocene field
443 models. *Phys Earth Planet In* **182**, 179-186 (2010).

444 24 Hoffman, K. A. & Singer, B. S. Magnetic source separation in Earth's outer core. *Science* **321**,
445 1800-1800 (2008).

446 25 Christensen, U. R. Geodynamo models: Tools for understanding properties of Earth's
447 magnetic field. *Phys Earth Planet In* **187**, 157-169 (2011).

448 26 Kutzner, C. & Christensen, U. R. Simulated geomagnetic reversals and preferred virtual
449 geomagnetic pole paths. *Geophys J Int* **157**, 1105-1118, doi:DOI 10.1111/j.1365-
450 246X.2004.02309.x (2004).

451 27 Buffett, B. A. in *Core Dynamics Vol. 8 Treatise on Geophysics* (ed P. Olson) Ch. 12, 345-358
452 (Elsevier, 2007).

453 28 Cande, S. C. & Kent, D. V. Revised Calibration of the Geomagnetic Polarity Timescale for the
454 Late Cretaceous and Cenozoic. *J Geophys Res-Sol Ea* **100**, 6093-6095 (1995).

455 29 Tominaga, M., Sager, W. W., Tivey, M. A. & Lee, S. M. Deep-tow magnetic anomaly study of
456 the Pacific Jurassic Quiet Zone and implications for the geomagnetic polarity reversal
457 timescale and geomagnetic field behavior. *J Geophys Res-Sol Ea* **113**, -,
458 doi:0.1029/2007jb005527 (2008).

459 30 Sager, W. W., Weiss, C. J., Tivey, M. A. & Johnson, H. P. Geomagnetic polarity reversal model
460 of deep-tow profiles from the Pacific Jurassic Quiet Zone. *J Geophys Res-Sol Ea* **103**, 5269-
461 5286 (1998).

462 31 Tominaga, M. & Sager, W. W. Revised Pacific M-anomaly geomagnetic polarity timescale.
463 *Geophys J Int* **182**, 203-232 (2010).

464 32 Gradstein, F. M., Ogg, J. G. & Smith, A. G. 589 (Cambridge University Press, Cambridge,
465 2004).

466 33 Ogg, J. G. in *A geological time scale 2004* (eds F. M. Gradstein, J. G. Ogg, & A. G. Smith)
467 307-339 (Cambridge University Press, 2004).

- 468 34 Ogg, J. G., Coe, A. L., Przybylski, P. A. & Wright, J. K. Oxfordian magnetostratigraphy of
469 Britain and its correlation to Tethyan regions and Pacific marine magnetic anomalies. *Earth*
470 *Planet Sc Lett* **289**, 433-448, doi:DOI 10.1016/j.epsl.2009.11.031 (2010).
- 471 35 Gee, J. S. & Kent, D. V. in *Geomagnetism Vol. 5 Treatise on Geophysics* (ed M Kono) Ch. 12,
472 455-507 (Elsevier, 2007).
- 473 36 He, H., Pan, Y., Tauxe, L., Qin, H. & Zhu, R. Toward age determination of the M0r
474 (Barremian–Aptian boundary) of the early Cretaceous. *Phys Earth Planet In* **169**, 41-48
475 (2008).
- 476 37 Granot, R., Tauxe, L., Gee, J. S. & Ron, H. A view into the Cretaceous geomagnetic field from
477 analysis of gabbros and submarine glasses. *Earth Planet Sc Lett* **256**, 1-11 (2007).
- 478 38 Tauxe, L. & Yamazaki, T. in *Geomagnetism Vol. 5 Treatise on Geophysics* (ed M Kono) Ch. 13,
479 510-563 (Elsevier, 2007).
- 480 39 Qin, H., He, H., Liu, Q. & Cai, S. Palaeointensity just at the onset of the Cretaceous normal
481 superchron. *Phys Earth Planet In* **187**, 199-211 (2011).
- 482 40 Tarduno, J. A. & Smirnov, A. V. in *Timescales of the Paleomagnetic Field Vol. 145 Geophysical*
483 *Monograph Series* (eds J. E. T. Channell, D.V. Kent, W. Lowrie, & J.G. Meert) 328 (AGU,
484 2004).
- 485 41 Granot, R., Dyment, J. & Gallet, Y. Geomagnetic field variability during the Cretaceous
486 Normal Superchron. *Nat Geosci* **5**, 220-223 (2012).
- 487 42 Prévot, M., Derder, M. E., McWilliams, M. & Thompson, J. Intensity of the Earths Magnetic-
488 Field - Evidence for a Mesozoic Dipole Low. *Earth Planet Sc Lett* **97**, 129-139 (1990).
- 489 43 Valet, J. P. Time variations in geomagnetic intensity. *Rev Geophys* **41**, 1004,
490 doi:10.1029/2001RG000104, doi:10.1029/2001RG000104 (2003).
- 491 44 Perrin, M. & Shcherbakov, V. Paleointensity of the earth's magnetic field for the past 400
492 Ma: Evidence for a dipole structure during the Mesozoic Low. *Journal of Geomagnetism and*
493 *Geoelectricity* **49**, 601-614 (1997).
- 494 45 Tarduno, J. A. & Cottrell, R. D. Dipole strength and variation of the time-averaged reversing
495 and nonreversing geodynamo based on Thellier analyses of single plagioclase crystals.
496 *Journal of Geophysical Research B: Solid Earth* **110**, 1-10 (2005).
- 497 46 McElhinny, M. W. & Larson, R. L. Jurassic Dipole Low Defined From Land and Sea Data. *Eos*
498 *Transactions AGU* **84**, 362, 310.1029/2003EO370003 (2003).
- 499 47 Biggin, A. J., van Hinsbergen, D., Langereis, C. G., G.B., S. & Deenen, M. H. L. Geomagnetic
500 Secular variation in the Cretaceous Normal Superchron and in the Jurassic. *Phys Earth Planet*
501 *In* **169**, 3-19 (2008).
- 502 48 McFadden, P. L. & Merrill, R. T. Evolution of the geomagnetic reversal rate since 160 Ma: Is
503 the process continuous? *J Geophys Res-Sol Ea* **105**, 28455-28460 (2000).
- 504 49 Langereis, C. G., Krijgsman, W., Muttoni, G. & Menning, M. Magnetostratigraphy - concepts,
505 definitions, and applications. *Newsl Stratigr* **43**, 207-233, doi:Doi 10.1127/0078-
506 0421/2010/0043-0207 (2010).
- 507 50 Pavlov, V. & Gallet, Y. A third superchron during the Early Paleozoic. *Episodes* **28**, 78-84
508 (2005).
- 509 51 Pavlov, V. & Gallet, Y. Middle Cambrian high magnetic reversal frequency (Kulumbe River
510 section, northwestern Siberia) and reversal behaviour during the Early Palaeozoic. *Earth*
511 *Planet Sc Lett* **185**, 173-183 (2001).
- 512 52 Kouchinsky, A. *et al.* The SPICE carbon isotope excursion in Siberia: a combined study of the
513 upper Middle Cambrian-lowermost Ordovician Kulyumbe River section, northwestern
514 Siberian Platform. *Geol Mag* **145**, 609-622, doi:Doi 10.1017/S0016756808004913 (2008).
- 515 53 Pavlov, V. & Gallet, Y. Variations in geomagnetic reversal frequency during the Earth's
516 middle age. *Geochem Geophys Geosy* **11**, doi:10.1029/2009gc002583 (2010).
- 517 54 Aubert, J., Labrosse, S. & Poitou, C. Modelling the palaeo-evolution of the geodynamo.
518 *Geophys J Int* **179**, 1414-1428, doi:10.1111/j.1365-246X.2009.04361.x (2009).

519 55 Driscoll, P. & Olson, P. Effects of buoyancy and rotation on the polarity reversal frequency of
520 gravitationally driven numerical dynamos. *Geophys J Int* **178**, 1337-1350 (2009).

521 56 Driscoll, P. & Olson, P. Superchron cycles driven by variable core heat flow. *Geophys Res Lett*
522 **38**, L09304 (2011).

523 57 Olson, P. Gravitational dynamos and the low-frequency geomagnetic secular variation. *P*
524 *Natl Acad Sci USA* **105**, 20159-20166 (2007).

525 58 Wicht, J., Stellmach, S. & Harder, H. in *Handbook of Geomathematics* (eds W. Freeden, M.Z.
526 Nashed, & T. Sonar) (Springer, 2010).

527 59 Olson, P. & Christensen, U. R. Dipole moment scaling for convection-driven planetary
528 dynamos. *Earth Planet Sc Lett* **250**, 561-571 (2006).

529 60 Pozzo, M., Davies, C., Gubbins, D. & Alfè, D. Thermal and electrical conductivity of iron at
530 Earth's core conditions. *Nature* **485**, 355-358 (2012).

531 61 Christensen, U. R. & Aubert, J. Scaling properties of convection-driven dynamos in rotating
532 spherical shells and application to planetary magnetic fields. *Geophys J Int* **166**, 97-114
533 (2006).

534 62 Glatzmaier, G. A., Coe, R. S., Hongre, L. & Roberts, P. H. The role of the Earth's mantle in
535 controlling the frequency of geomagnetic reversals. *Nature* **401**, 885-890 (1999).

536 63 Olson, P. L., Coe, R. S., Driscoll, P. E., Glatzmaier, G. A. & Roberts, P. H. Geodynamo reversal
537 frequency and heterogeneous core-mantle boundary heat flow. *Phys Earth Planet In* **180**,
538 66-79 (2010).

539 64 Pétrélis, F., Fauve, S., Dormy, E. & Valet, J. P. Simple Mechanism for Reversals of Earth's
540 Magnetic Field. *Phys Rev Lett* **102**, doi:10.1103/Physrevlett.102.144503 (2009).

541 65 Wicht, J., Stellmach, S. & Harder, H. in *Geomagnetic field variations – Space–time structure,*
542 *processes, and effects on system Earth.* (eds K. H. Glassmeier, H. Soffel, & J. Negendank)
543 107-158 (Springer, 2009).

544 66 Lay, T., Hernlund, J. & Buffett, B. A. Core-mantle boundary heat flow. *Nat Geosci* **1**, 25-32,
545 doi:Doi 10.1038/Ngeo.2007.44 (2008).

546 67 van der Hilst, R. D. *et al.* Seismostratigraphy and thermal structure of Earth's core-mantle
547 boundary region. *Science* **315**, 1813-1817 (2007).

548 68 Garnero, E. J., Lay, T. & McNamara, A. in *Plates, plumes, and planetary processes* Vol. 430
549 *Geological Society of America Special Paper* (eds G.R. Foulger & D.M. Jurdy) 79-101 (2007).

550 69 Machel, P. & Thomassot, E. Cretaceous length of day perturbation by mantle avalanche.
551 *Earth Planet Sc Lett* **202**, 379-386 (2002).

552 70 Fukao, Y., Widiyantoro, S. & Obayashi, M. Stagnant slabs in the upper and lower mantle
553 transition region. *Rev Geophys* **39**, 291-323 (2001).

554 71 Van der Voo, R., Spakman, W. & Bijwaard, H. Mesozoic subducted slabs under Siberia.
555 *Nature* **397**, 246-249 (1999).

556 72 vanderHilst, R. D., Widiyantoro, S. & Engdahl, E. R. Evidence for deep mantle circulation from
557 global tomography. *Nature* **386**, 578-584 (1997).

558 73 Grand, S. P., Van der Hilst, R. D. & Widiyantoro, S. Global seismic tomography: A snapshot of
559 convection in the Earth. *GSA Today* **7**, 1-7 (1997).

560 74 Goes, S., Capitanio, F. A. & Morra, G. Evidence of lower-mantle slab penetration phases in
561 plate motions. *Nature* **451**, 981-984 (2008).

562 75 Steinberger, B. M. & Torsvik, T. H. A geodynamic model of plumes from the margins of Large
563 Low Shear Velocity Provinces. *Geochem Geophys Geosy*, doi:10.1029/2011GC003808 (2012).

564 76 Čížková, H., van den Berg, A. P., Spakman, W. & Matyska, C. The viscosity of Earth's lower
565 mantle inferred from sinking speed of subducted lithosphere,. *Phys Earth Planet In in press.*,
566 10.1016/j.pepi.2012.1002.1010 (2012).

567 77 Labrosse, S. Hotspots, mantle plumes and core heat loss. *Earth Planet Sc Lett* **199**, 147-156
568 (2002).

569 78 Gonnermann, H. M., Jellinek, A. M., Richards, M. A. & Manga, M. Modulation of mantle
570 plumes and heat flow at the core mantle boundary by plate-scale flow: results from
571 laboratory experiments. *Earth Planet Sc Lett* **226**, 53-67, doi:DOI 10.1016/j.epsl.2004.07.021
572 (2004).

573 79 Nakagawa, T. & Tackley, P. J. Deep mantle heat flow and thermal evolution of the Earth's
574 core in thermochemical multiphase models of mantle convection. *Geochem Geophys Geosy* **6**,
575 doi:Artn Q08003

576 Doi 10.1029/2005gc000967 (2005).

577 80 Thorne, M. S., Garnero, E. J. & Grand, S. P. Geographic correlation between hot spots and
578 deep mantle lateral shear-wave velocity gradients. *Phys Earth Planet In* **146**, 47-63 (2004).

579 81 Tan, E., Leng, W., Zhong, S. J. & Gurnis, M. On the location of plumes and lateral movement
580 of thermochemical structures with high bulk modulus in the 3-D compressible mantle.
581 *Geochem Geophys Geosy* **12** (2011).

582 82 Burke, K., Steinberger, B., Torsvik, T. H. & Smethurst, M. A. Plume generation zones at the
583 margins of large low shear velocity provinces on the core-mantle boundary. *Earth Planet Sc*
584 *Lett* **265**, 49-60 (2008).

585 83 Burke, K. Plate Tectonics, the Wilson Cycle, and Mantle Plumes: Geodynamics from the Top.
586 *Annu Rev Earth Pl Sc* **39**, 1-29, doi:DOI 10.1146/annurev-earth-040809-152521 (2011).

587 84 Larson, R. L. Latest Pulse of Earth - Evidence for a Midcretaceous Superplume. *Geology* **19**,
588 547-550 (1991).

589 85 Bryan, S. E. & Ernst, R. E. Revised definition of large igneous provinces (LIPs). *Earth-Sci Rev*
590 **86**, 175-202, doi:DOI 10.1016/j.earscirev.2007.08.008 (2008).

591 86 Olson, P., Schubert, G. & Anderson, C. Plume Formation in the D''-Layer and the Roughness
592 of the Core Mantle Boundary. *Nature* **327**, 409-413 (1987).

593 87 Thompson, P. F. & Tackley, P. J. Generation of mega-plumes from the core-mantle boundary
594 in a compressible mantle with temperature-dependent viscosity. *Geophys Res Lett* **25**, 1999-
595 2002 (1998).

596 88 van Hinsbergen, D. J. J., Steinberger, B., Doubrovine, P. V. & Gassmoller, R. Acceleration and
597 deceleration of India-Asia convergence since the Cretaceous: Roles of mantle plumes and
598 continental collision. *J Geophys Res-Sol Ea* **116** (2011).

599 89 Gold, T. Instability of the Earths Axis of Rotation. *Nature* **175**, 526-529 (1955).

600 90 Steinberger, B. & Torsvik, T. H. Toward an explanation for the present and past locations of
601 the poles. *Geochem Geophys Geosy* **11**, - (2010).

602 91 Tsai, V. C. & Stevenson, D. J. Theoretical constraints on true polar wander. *J Geophys Res-Sol*
603 *Ea* **112** (2007).

604 92 Steinberger, B. & Torsvik, T. H. Absolute plate motions and true polar wander in the absence
605 of hotspot tracks. *Nature* **452**, 620-U626 (2008).

606 93 Mitchell, R. N., Kilian, T. M. & Evans, D. A. D. Supercontinent cycles and the calculation of
607 absolute palaeolongitude in deep time. *Nature* **482**, 208-U296, doi:Doi
608 10.1038/Nature10800 (2012).

609 94 Torsvik, T. H. *et al.* Phanerozoic polar wander, paleogeography and dynamics. *Earth-Sci Rev*
610 (submitted).

611 95 Becker, T. W. & Boschi, L. A comparison of tomographic and geodynamic mantle models.
612 *Geochem Geophys Geosy* **3**, - (2002).

613 96 Tan, E., Gurnis, M. & Han, L. J. Slabs in the lower mantle and their modulation of plume
614 formation. *Geochem Geophys Geosy* **3** (2002).

615 97 Biggin, A., McCormack, A. & Roberts, A. Paleointensity Database Updated and Upgraded.
616 *Eos, Transactions American Geophysical Union* **91**, 15 (2010).

617 98 Thellier, E. & Thellier, O. Sur l'intensité du champ magnétique terrestre dans la passé
618 historique et géologique. *Ann. Géophys.* **15**, 285-376 (1959).

619 99 Hill, M. J. & Shaw, J. Magnetic field intensity study of the 1960 Kilauea lava flow, Hawaii,
620 using the microwave palaeointensity technique. *Geophys J Int* **142**, 487-504 (2000).
621 100 Yamamoto, Y., Tsunakawa, H. & Shibuya, H. Palaeointensity study of the Hawaiian 1960 lava:
622 implications for possible causes of erroneously high intensities. *Geophys J Int* **153**, 263-276
623 (2003).

624

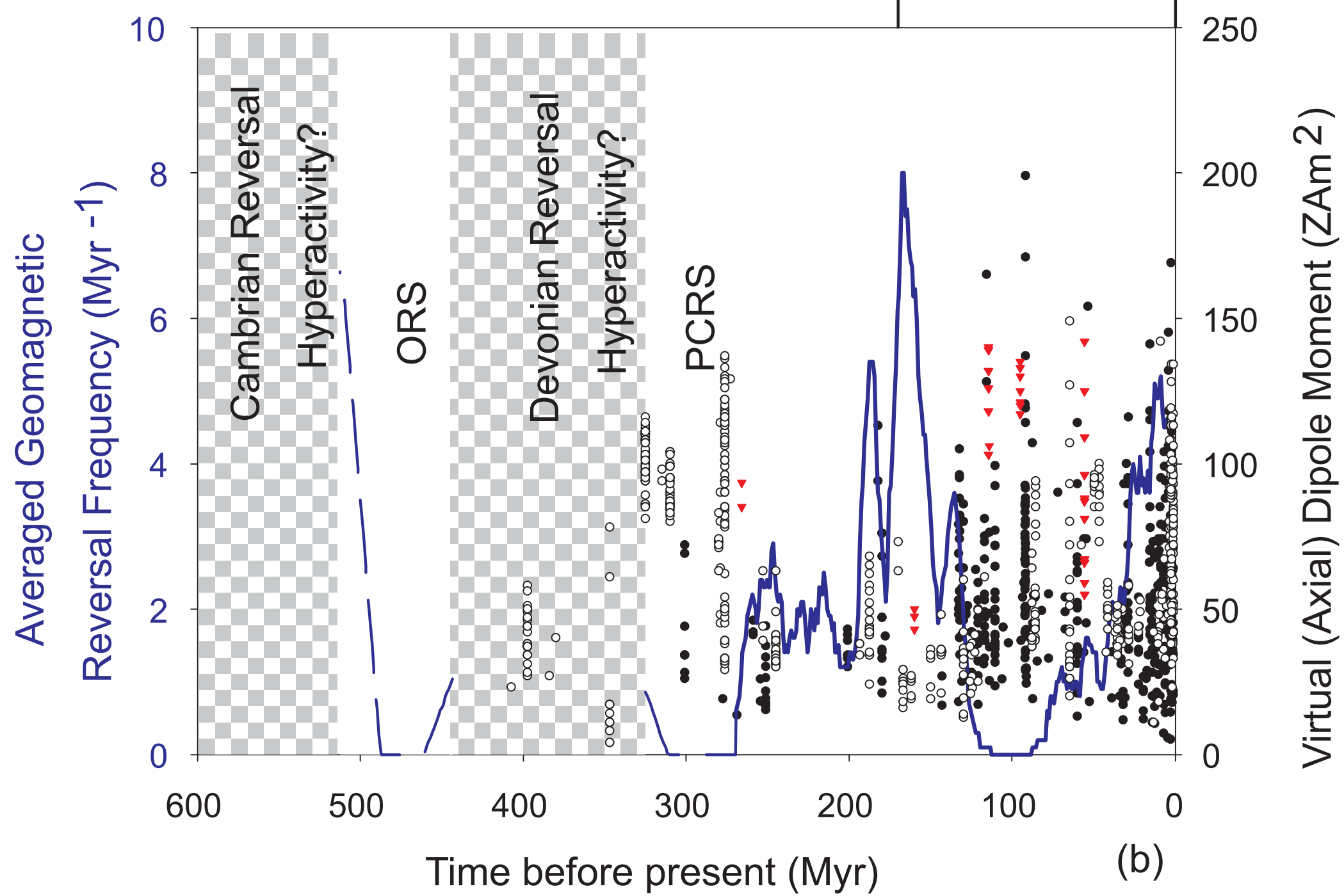
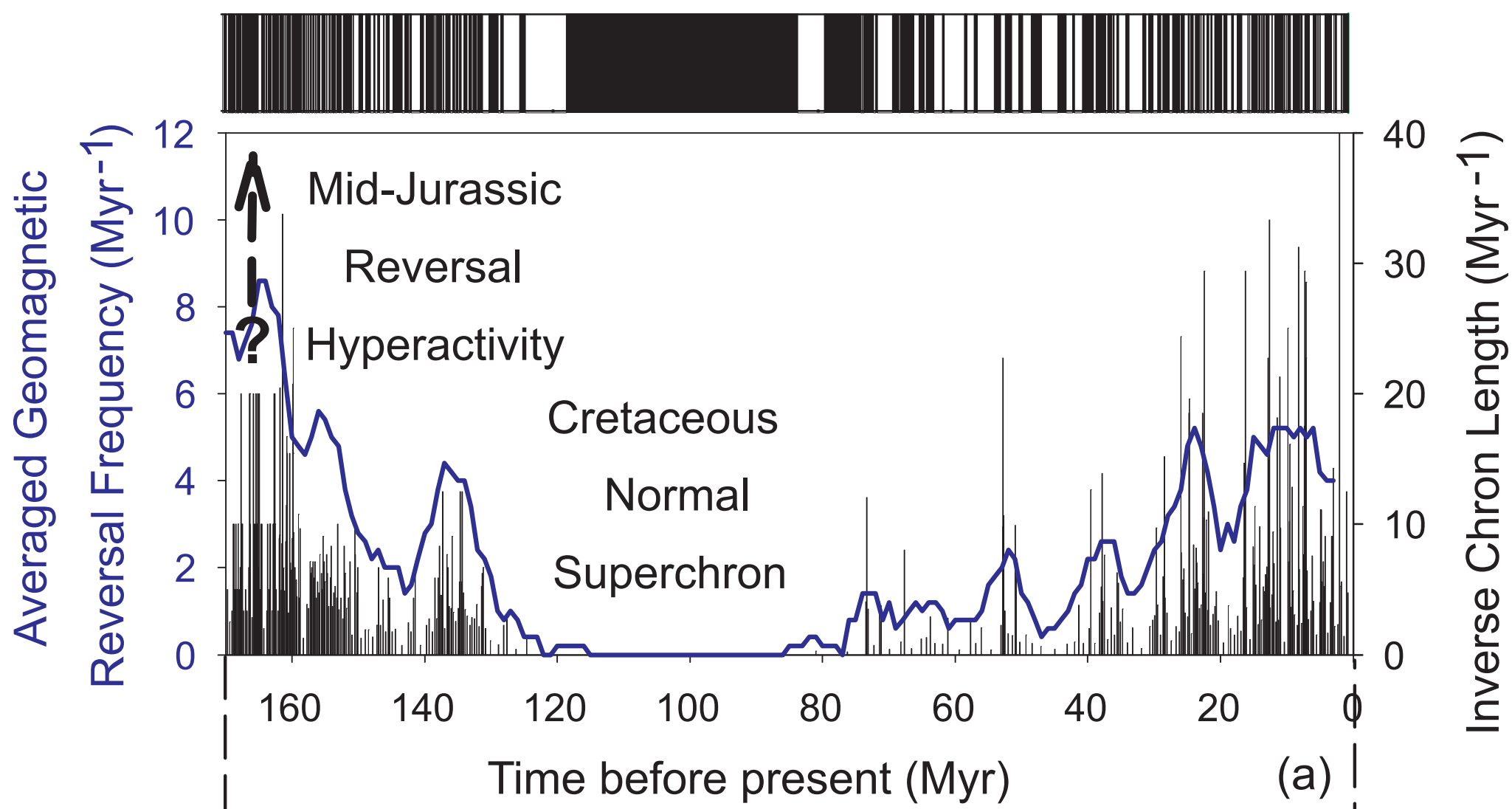
625 **Figure 1:** Records of geomagnetic polarity reversal frequency and dipole moment since the
626 Cambrian. (a) The marine magnetic anomaly record (MMA)²⁸⁻³¹ and plots of inverse chron
627 length (black bars) and reversal frequency (10 Myr running mean; blue line). (b) Reversal
628 frequency from the MMA and magnetostratigraphic studies³³ (chequered area indicates
629 insufficient data) alongside virtual (axial) dipole moment (spatially-normalised field intensity)
630 measurements⁹⁷ from single silicate crystals (red triangles) and whole rocks (filled circles for
631 Thellier⁹⁸ or microwave methods⁹⁹ with pTRM checks and the LTD-DHT Shaw¹⁰⁰ method;
632 unfilled circles for other methods; $N \geq 3$; $\sigma/\mu \leq 0.25$ in all cases).

633 **Figure 2:** Representative cases of a mantle flow model showing the effects of subducted slabs
634 on CMB heat flow. (a) CMB heat flow increases ~ 50 Myr after subduction begins (Cases 2 and 3)
635 but is still decreasing ~ 300 Myr after subduction ends (Case 1); (b) the slab (blue) marked with
636 the asterisk interacts with a plume (red/white) and remains as a positive density anomaly after
637 250 Myr; (c) CMB heat flow at present-day (reversal frequency $\sim 4 \text{ Myr}^{-1}$) is greater at
638 equatorial latitudes and more asymmetric about the equator than during the superchron at 100
639 Ma.

640 **Figure 3:** Average reversal frequency and eruption ages²⁰ of LIPs (offset by +50 Myr) that have
641 not yet been subducted. Mantle plume-heads leaving the CMB may reflect enhanced heat flow
642 out of the core potentially increasing reversal frequency tens of Myr before the resulting
643 eruption of the LIPs. Allowing for an average rise-time of 50 Myr produces a broad correlation
644 that would associate geomagnetic reversal hyperactivity in the mid-Jurassic with widespread
645 LIP emplacement in the mid-Cretaceous. In the period 0-50 Myr, mantle plume heads which had
646 left the CMB would not yet have reached the surface.

647 **Figure 4:** TPW as produced by a mantle flow model (Case 2) subject to two major perturbations
648 in subduction flux which affected the fractional CMB heat flow in the equatorial region. (a) The
649 geographic pole through time (Myr before present) shown on stereographic projections
650 featuring present-day landmasses for reference. (b) Time series of the fraction of global CMB
651 heat flow between 10°N and 10°S. Differences between the heat flow in the two reference
652 frames is due to TPW which first maximises and then minimises its equatorial fraction and
653 could similarly affect reversal frequency.

654 **Figure 5:** Analysis of possible effects of observed TPW on equatorial CMB heat flow (and hence
655 reversal frequency). (a) Rotated examples of the SMEAN tomographic model⁹⁵. Higher shear
656 wave velocities (red areas) are likely to be associated with lower temperatures and higher CMB
657 heat flux. (b) Model of TPW for the last 300 Myr⁹⁴. (c) Resulting time series (red line) of
658 variations in average shear wave velocity (inferring relative changes in heat flow) in the
659 equatorial region (between 10°N and 10°S) shown alongside reversal frequency (black line).



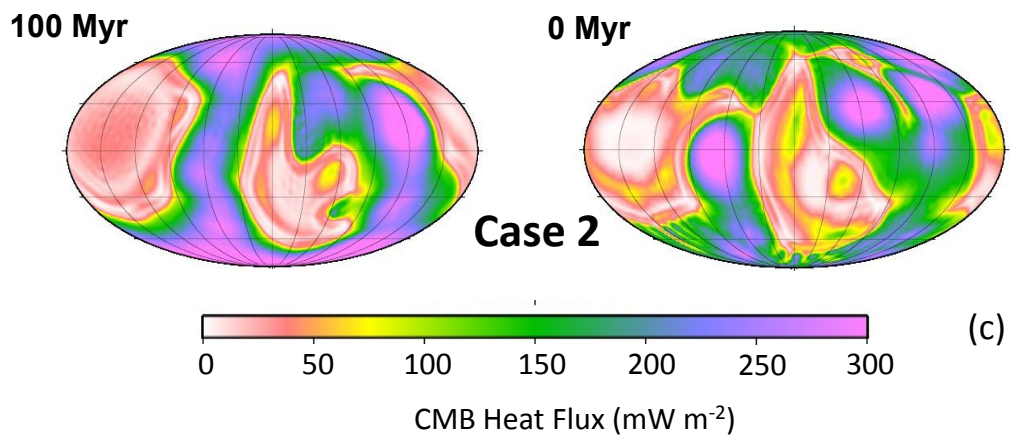
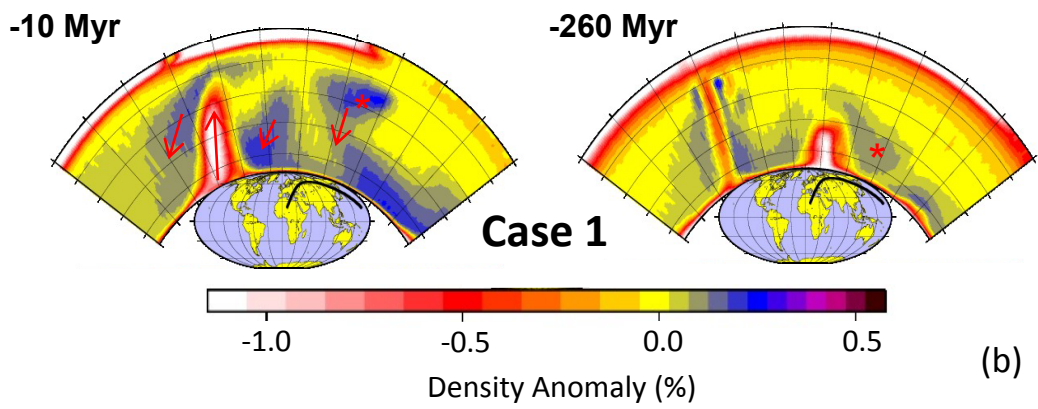
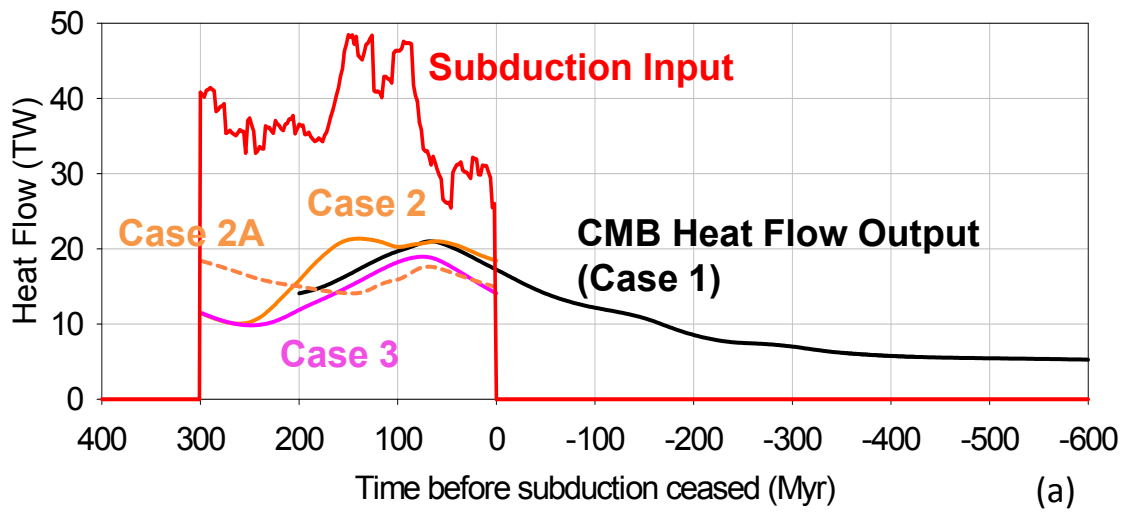
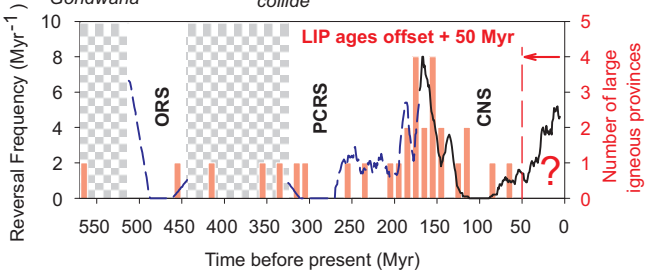


Figure 2

*Terminal
formation of
Gondwana*

*Laurussia and
Gondwana
collide*



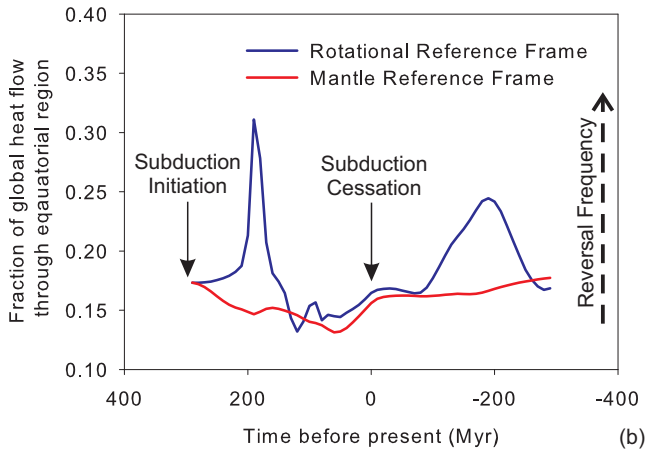
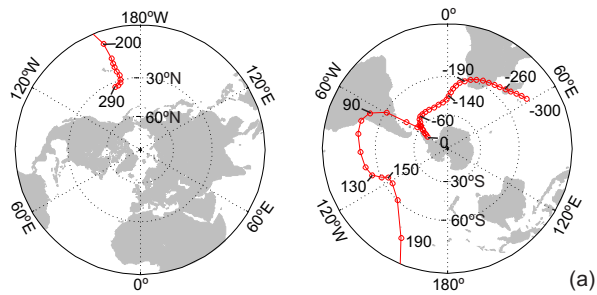


FIGURE 4

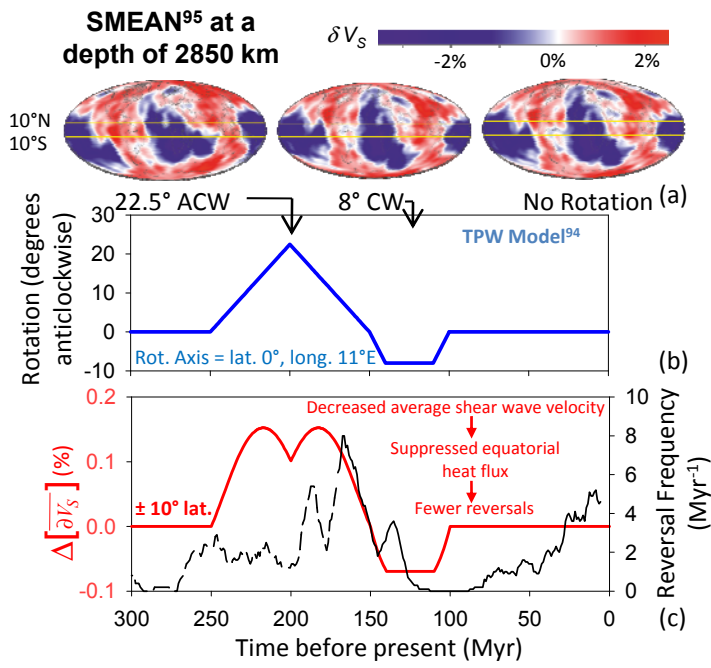


FIGURE 5